Microwave Line-of-Sight Propagation With and Without Frequency Diversity

By W. T. BARNETT

(Manuscript received May 5, 1970)

Amplitude measurements were made for 68 days in 1966 for seven 4-GHz and 6-GHz signals on a typical radio relay path. Identical measurements were also made for one 4-GHz signal on a second path having a common reception point with the first path. We present the results from an analysis centered on the fade-depth distribution for fades exceeding 20 dB. The more significant results are:

(i) The fade-depth distribution for all single (nondiversity) channels in a 5-10 percent band on the same path are essentially the same. Further, the distribution has the Rayleigh slope.

(ii) The single-channel fade-depth distributions differ for 4 and 6 GHz on the same path; the distributions also differ for the same 4-GHz frequency on adjacent paths with a common reception point.

(iii) One-for-one frequency diversity can be characterized during multipath fading periods for either the 4- or 6-GHz bands by the ratio of two quantities. The first is the precent frequency separation between diversity components. The second is the nondiversity fade-depth distribution.

I. INTRODUCTION

Line-of-sight microwave systems are affected by multipath propagation. When this phenomenon is present, the output from a receiving antenna can be practically zero for seconds at a time. Experimental data are difficult to obtain because long time periods of continuous coverage are needed to observe sufficient fading activity at the fade depths (30–40 dB) of interest for high performance systems. The literature is extensive on this general topic[1–7] but limited and in some cases contradictory[8] for these fade depths. The results available regarding frequency diversity are even more limited[9]. For these and other reasons, an extensive experimental program was undertaken in 1966.

Continuous amplitude measurements were made for 68 days at a rate of 5 samples per second per channel for seven 4-GHz and six 6-GHz signals on a radio relay path at West Unity, Ohio. Identical measurements were also made for one 4-GHz signal on a second path having a common reception point with the first path. Here a 68-day summer period (July 22 to September 28) in 1966 has been subjected to detailed analysis.

We present the results of the data analysis and their interpretation along with pertinent background information. Briefly the order of presentation is (*i*) experiment description, (*ii*) determination of the reference values used for calibration, (*iii*) nondiversity results, (*iv*) frequency diversity results, (*v*) a mathematical description of pairwise fading which is used to interpret the improvement obtained from frequency diversity, (*vi*) 4/6 GHz crossband results, (*vii*) adjacent hop results, and (*viii*) a comparison of space and frequency diversity.

II. SUMMARY

New results have been obtained from the data concerning 4- and 6-GHz propagation on line-of-sight paths. The present analysis was centered on the fade-depth distribution for fades of 20 dB or more. A simplified listing of the significant findings follows.

(*i*) During nonfading conditions, the received microwave signal power was constant for the entire test period to within ±1 dB including equipment variations.

(*ii*) The fade-depth distributions for all single (nondiversity) channels in a 5-10 percent band are essentially the same and have a Rayleigh slope.

(*iii*) The single-channel fade-depth distributions differ for 4 and 6 GHz on the same path; the distributions also differ for the same 4-GHz frequency on adjacent paths with a common reception point.

(*iv*) The performance of a one-for-one frequency diversity system can be specified for either the 4- or 6-GHz bands by the ratio of two quantities. The first is the percent frequency separation ($100\ \Delta f/f$) between in-band diversity signal components. The second is the experimental nondiversity fade-depth distribution $P(L)$. In these terms the improvement (I) of a diversity system relative to the nondiversity system as obtained from the data is simply

$$I = 0.13 \frac{\Delta f}{f} \Big/ P(L).$$

This model is based upon the in-band frequency diversity data and is in agreement therewith.

The factor I characterizes frequency diversity during multipath fading periods. As such, it should be applicable to different climates and terrains for path lengths of approximately 28 miles.

(*v*) The improvement from 4/6 GHz crossband diversity was not significantly better than in-band diversity of 2 percent or more separation.

(*vi*) Adjacent section diversity with a common point (as based on data on a single channel) was not significantly better than in-band frequency diversity. This raises some provoking (unanswered) questions about the correlation of selective fading on adjacent routes, for example, limitations on the maximum possible diversity improvement to values less than those expected from independent fading.

(*vii*) The performance of space diversity[10] is comparable to that of one-for-one frequency diversity on the same hop.

(*viii*) The polarization of the radio signals had no noticeable effect on the amount of fading.

These results are presented in detail along with the necessary background information in the following sections.

III. EXPERIMENT DESCRIPTION

The transmitted power in microwave radio systems is constant. Propagation data can therefore be obtained from in-service systems without interfering with their operation by using suitable monitoring equipment. Such equipment (MIDAS*) was installed at West Unity, Ohio, to monitor and record the received envelope voltages of standard TD-2 (4 GHz) and TH(6 GHz) signals. A list of the channels is given on Table I. Briefly there were seven 4-GHz, six 6-GHz, and two space-diversity channels on one hop and one 4-GHz channel on a second hop. A functional block diagram is shown on Fig. 1.

West Unity, Ohio, was chosen as the measuring site for this experiment because it lies along a major route in an area with a reputation for considerable fading. Further, the hops measured have average lengths (28.5 and 29.4 miles) with negligible ground reflections. The two paths differ in azimuth by 68 degrees and their profiles are given on Figs. 2 and 3; clearance is adequate even for the extreme case of equivalent earth radius (k) equal to two-thirds.

* An acronym for Multiple Input Data Acquisition System.

TABLE I—RADIO CHANNELS MEASURED AT WEST UNITY, OHIO

Channel No.	Frequency	Antenna	Polarization
From Pleasant Lake, Indiana (28.5 mi)			
4-7	3750	Horn Reflector	V
4-1	3770		H
4-8	3830		V
4-2	3850		H
4-9	3910		V
4-11	4070		V
4-6	4170		H
6-11	5945.2		H
6-13	6004.5		H
6-14	6034.2		V
6-15	6063.8		H
6-17	6123.1		H
6-18	6152.8		V
6-UD	6152.8	Upper Dish	V
6-LD	6152.8	Lower Dish	V
From Paulding, Ohio (29.4 mi)			
4-6	4170	Horn Reflector	V

Note: The 4-*X* channels correspond to standard TD-2 radio system signals; 6-*X* corresponds to TH.

The MIDAS equipment derived received signal strength information by sampling the voltage of the 70-MHz IF signal at a point where it was linearly related to the RF signal. At any instant the particular channel being measured was selected automatically by MIDAS. A common detector then converted the IF amplitude measurement to a dc voltage which was quantized into one of 32 contiguous steps over a 45-dB range. The MIDAS input-output curve is given as Fig. 4.

The data were recorded on paper tape along with the necessary timing information. Measurements were made throughout the 68-day period at a rate of 5 samples per second on each channel. The information was recorded for all channels at rates of either 1 sample per 30 seconds, 1 sample per 2 seconds and 5 samples per second (normal, intermediate, and fast rates) depending on the fading activity of the channels under test. The recording rate was automatically selected by MIDAS so as to record all significant fading. During computer processing of the data, the amplitude value at a sampling instant was assumed to hold until the next sampling instant.

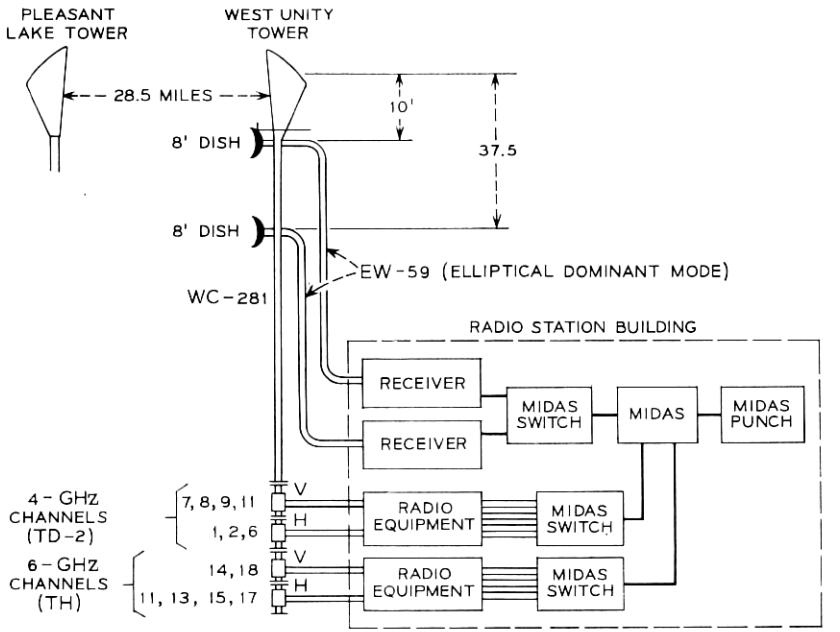

Fig. 1—Experimental layout, Pleasant Lake to West Unity (Paulding to West Unity not shown).

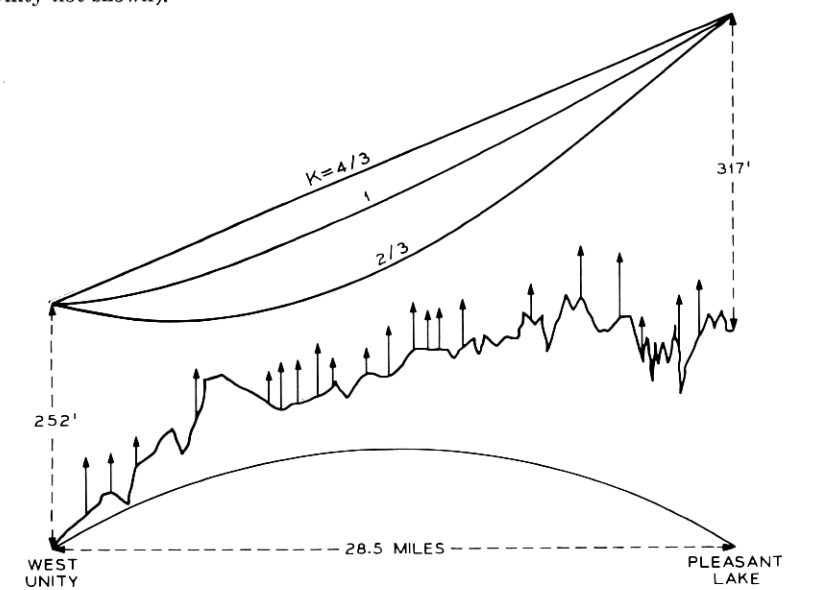

Fig. 2—West Unity—Pleasant Lake path profile.

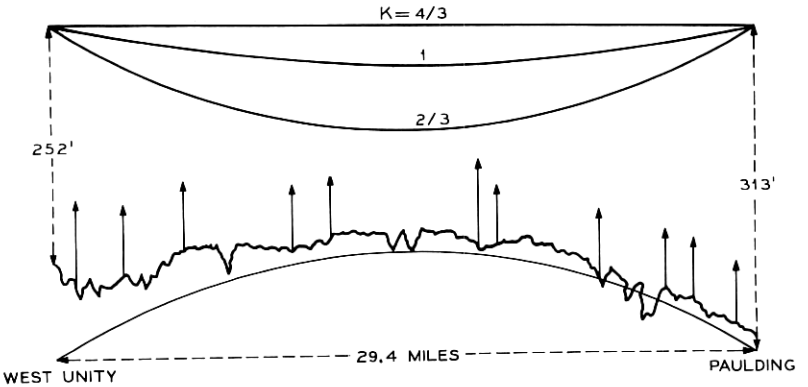

Fig. 3—West Unity—Paulding, Ohio, path profile.

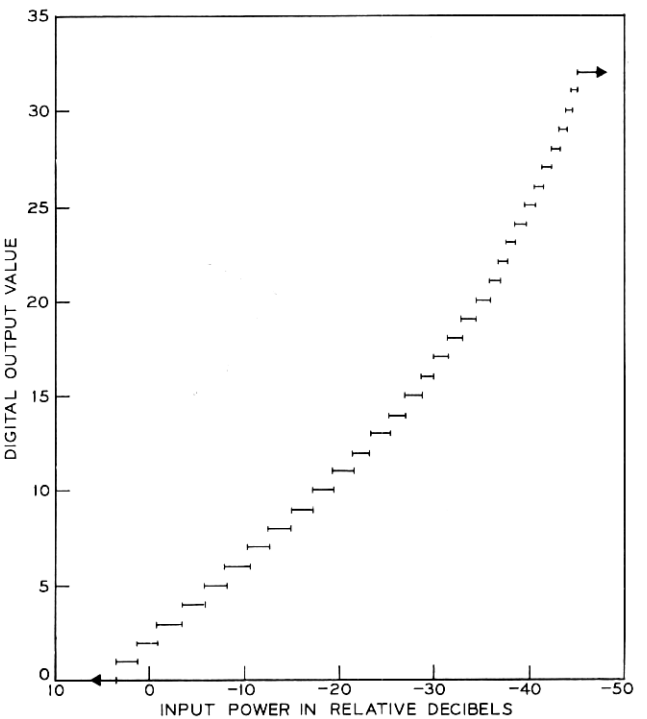

Fig. 4—MIDAS calibration curve.

An important feature of the experiment was long-term continuous coverage. Deep fades are rare events occurring at unpredictable times; the test equipment had to be on-line continuously to obtain an adequate sample.

The required test equipment reliability and measurement uniformity was obtained by maximum use of common equipment. The essentially continuous coverage was obtained by recording mainly the significant fading data. Even so the subsequent processing was a formidable task, even with the computer, because of the high volume of raw data.

IV. NONFADING SIGNAL VALUES

A fade is defined as a decrease in the envelope of the received signal voltage with respect to a reference or free-space value. Thus before fading data can be quantified, the reference or nonfading value must be determined.

If the atmosphere between the transmitting and receiving antennas was homogeneous (that is, no vertical or horizontal variations in the index of refraction), then the single frequency RF power at the output of the receiving antenna would be invariant for a fixed transmitted power.* Its value (called the free-space value) could be calculated in a straightforward manner. However, even during nonfading periods, there are small time-varying random deviations in the refractive index which cause small scintillations in the received power even when the average value remains constant. There are also long-term variations in the received RF power due to equipment variation. For our purposes we must determine the nonfaded received power as a function of time and, if possible, quantify the scintillations.

Inspection of the data showed that the midday hours had the least amount of fading. Here the differentiation between fading and free-space scintillations is made on the basis of the magnitude of the effect. Fading causes variations of one or more quantizing levels in the envelope from hour-to-hour on most of the 15 channels.

To establish a reference value, midday periods were sought which had no fading with respect to either time or frequency. It was easy to find a total of 129 midday hours simultaneously for all channels on 30 different days scattered throughout the entire 68-day period.

Table II gives the summaries for the midday values. The table shows the average signal in terms of quantizing level for five consecutive time periods of from 9 to 20 days duration. Several points can be made about

* Assuming adequate ground clearance and no ground reflections.

TABLE II—AVERAGE NONFADED VALUES
(in terms of quantizing levels)

	Time Periods				
	1	2	3	4	5
Pleasant Lake					
4- 7	4	4	4.5	4	4.5
- 1	2	2	2	1.5	1.5
- 8	3	3	3	2.5	2.5
- 2	3	3	2.5	3	3
- 9	4	4	4	4	4
-11	4	4	4	4	3.5
- 6	4	3.5	3.5	3.8	3.5
6-11	2	1.5	2	1.5	1.4
-13	2	2	2	1	1
-14	2	2	2	2	2
-15	1	1	1.5	1	1
-17	2	2	2	2	2
-18	2	1.5	2	2	1.5
6-UD	4	3.5	3.5	3.8	3.5
6-LD	5	4.5	5	4.5	4.2
Paulding					
4- 6	2	2	2	3	2.8
Total Hours in Period	254	375	482	264	263
Hours Used	31	22	24	25	27
Total Days in Period	9	16	20	11	12
Days Used	7	7	7	5	4

Note: Quantizing level 4.X means that the average value was 0.X of a level offset from the center of level 4 in the direction of level 5.

this data. First the maximum peak-to-peak variation on any channel is one level or about 2 dB while the average variation is $\pm\frac{1}{4}$ of a level or about ± 0.5 dB. Further some of the channels, for example, 4-1 and 6-13, exhibit a definite trend over the 129 hours. The belief is that these long-term effects are attributable to the radio equipment.

In any case, the average deviation of ± 0.5 dB is small enough so that a single reference value for each channel can be used for the entire time period. This simplifies data reduction considerably.

Now consider the statistics of small scintillations in the received signal

power. Table III gives the percent distributions by level for all the channels for the 129 midday hours. Of course this distribution includes the long-term equipment variations in the reference values as well as the short-term scintillations. Note that the channels with the minimum variations in average value from Table II are those with most of their "90 percent hours" in a single level. These are 4-9, 4-11, 6-14, and 6-17. It is assumed that the variations on these channels are due *only* to scintillation and that this effect can be represented by a probability distribution which is normal in dB. The σ of this distribution can be found from the percent values given in Table III with the results shown in Table IV. The agreement between these channels is excellent. The conclusion is that the scintillation effect over a 68-day period is universal with a σ of 0.6 dB superimposed on an equipment variation of ± 0.5 dB. The rms variation in reference value is then ± 0.8 dB.

4.1 *Channel Calibration*

The data on reference values were combined with the MIDAS calibration curve to calibrate the 15 RF channels in dB. First, all the 6- and 4-

TABLE III—SUMMARY OVER ENTIRE 68 DAYS
(Data for 129 Hours on 30 Days)

Channel Freq.	Percent of Time in Level					Hours with 90 Percent or More of Time in Level				
	1	2	3	4	5	1	2	3	4	5
West Unity										
4- 7			0.32	78.25	21.43				63	
- 1	18.1	80.50	1.40			12	93			
- 8		17.52	81.34	1.13	0.01		9	88		
- 2		0.01	86.25	13.74				95		
- 9			7.41	91.94	0.65			1	111	
-11			10.36	88.93	0.71				96	
- 6		0.77	32.50	66.73			1	16	58	
6-11	28.57	69.60	1.83			9	47			
-13	34.56	63.68	1.76			31	71			
-14	6.01	92.65	1.34			4	118			
-15	83.95	16.01	0.04			94	6			
-17	2.10	94.96	2.94				113			
-18	17.88	78.96	3.16			4	69	1		
6-UD			34.65	65.27	0.08			18	42	8
6-LD				33.2	66.80				24	66
Paulding 4- 6	4.09	58.04	37.87			2	59	42		

TABLE IV—LONG-TERM STANDARD DEVIATION

Channel	σ in dB
4-9	0.56
4-11	0.59
6-14	0.58
6-17	0.56

GHz channels were simultaneously lined up at their reference level which was specified as 0 dB. By inspection, 29 dB values were chosen over the fading range in order to give minimum ambiguity over the entire set of channels; thus each quantizing step on each channel was not used more than once. In this way all the 6- and 4-GHz channels were simultaneously calibrated; this was done so that an arbitrary subset could be chosen for analysis without having to recalibrate. Figure 5 gives an example of the results of the calibration procedure for channels 4-7, 4-2, and 4-9 for fades greater than 20 dB.

Because the calibration curve is nonlinear, this process requires some judgment. The minor combined effects of the nonlinear calibration

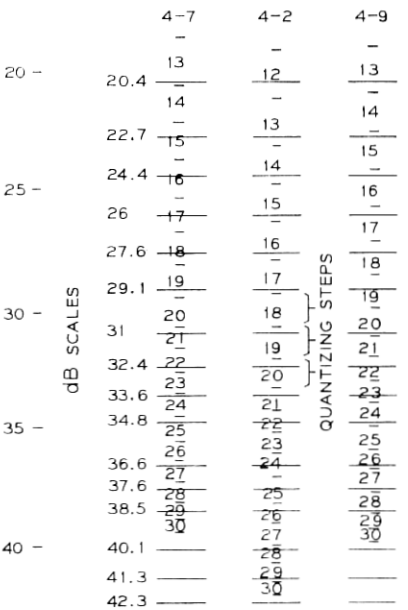

Fig. 5—Calibration example.

curve and differing reference levels for different channels are discussed in conjunction with the single channel outage statistics.

V. SINGLE CHANNEL RESULTS

The raw data were obtained continuously for almost all of the 68 days (5.9×10^6 seconds). Of this total, 5.26×10^6 seconds was used as the data base; the balance was lost mainly because of routine radio maintenance. To condense the data, a criterion was used to select by computer only those time periods which exhibited fading. The start of such a time period was defined by, and included, ten consecutive measurements containing any one channel faded below approximately 10 dB. The end of the time period was defined as that instant for which the next 110 consecutive measurements on any channel did not have a fade exceeding approximately 10 dB.

From the total of 5.26×10^6 seconds, 7.8×10^5 seconds (14.8 percent) were selected for analysis. The average length of the periods selected was sizeable. There were only 96 distinct periods selected; these had an average length of 8.1×10^3 seconds ($2\frac{1}{4}$) hours.) Further one-half of the analysis time was in intervals of four hours or longer. Thus any effects due to beginning or ending a time period should be minimal.

The data were processed by computer to determine the total amount of time during which each signal was less than a certain amount. The 4-GHz single-channel fading results are given on Fig. 6 for fades greater than 20 dB. These results and all those to follow are given as a fraction of 5.26×10^6 seconds. It is apparent that these statistics are essentially the same for all the 4-GHz channels and have the Rayleigh slope, that is, 10 dB per decade of probability over the entire range of data points. The solid line on the figure is a least-square fit of a Rayleigh slope line to the data points, most of which are within ± 1 dB as shown by the dashed lines. This scatter is due to both the uncertainties in the reference value and to the nonlinear calibration.

The 4-2 points outside the 2-dB corridor from 22 to 29 dB are due to the nonlinear quantized calibration. From Fig. 5 note that for 4-2 the dB values used lie near the bottom of the quantizing levels up to 31 dB at which point they change to the middle of the quantizing levels. This gives the effect noted on Fig. 6, that is, the data points are shifted to higher fade values for a constant probability. Other anomalies of this type in the single-channel results are explainable in this manner. For these results and for all others described here, the polarization of the signal (s) had no apparent effect.

The 6-GHz signal channel results are given on Fig. 7 for fades greater

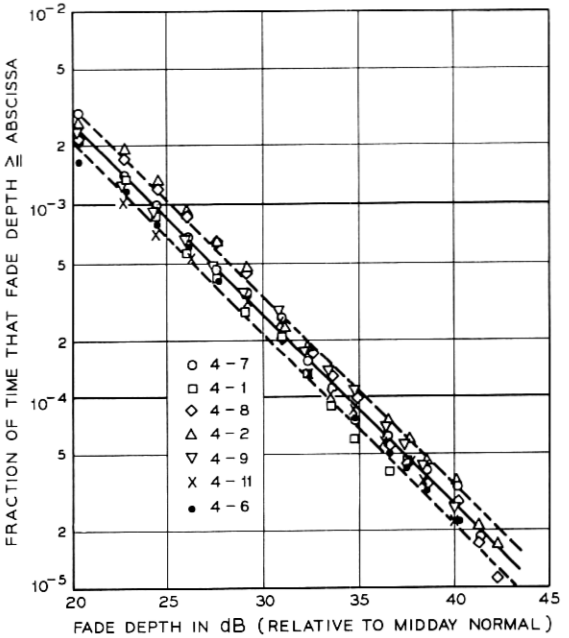

Fig. 6—Fade-depth distribution; 4-GHz channels.

than 20 dB. Again all 6-GHz channels have essentially the same statistics with the solid line being the least-squares fit with a Rayleigh slope. Almost all data points are within ±1 dB of the average above 40 dB except for 6-15 from 37 to 40 dB. This discrepancy is attributable to nonlinear quantizing as discussed for 4 GHz. The increased scatter above 40 dB is thought to be due to decreasing measurement sensitivity.

The single-channel results for the space diversity grouping[10] (the 6-18 signal is received on the horn reflector and two dishes) and for the 4-GHz channel on the Paulding route are given on Fig. 8. The lines are the least-squares fit with a Rayleigh slope.

Figure 9 gives a summary of the single-channel statistics and for comparison, the true Rayleigh curve. The equations of the least-square lines are

West Unity	4:	$P = 0.25\ 10^{-F/10}$
	6:	$P = 0.53\ 10^{-F/10}$
	SD:	$P = 0.43\ 10^{-F/10}$
Paulding	4:	$P = 0.77\ 10^{-F/10}$

where F is the fade depth expressed in dB ($F \geqq 20$ dB). The channel with the most fading was the 4-GHz Paulding followed by 6 GHz, space

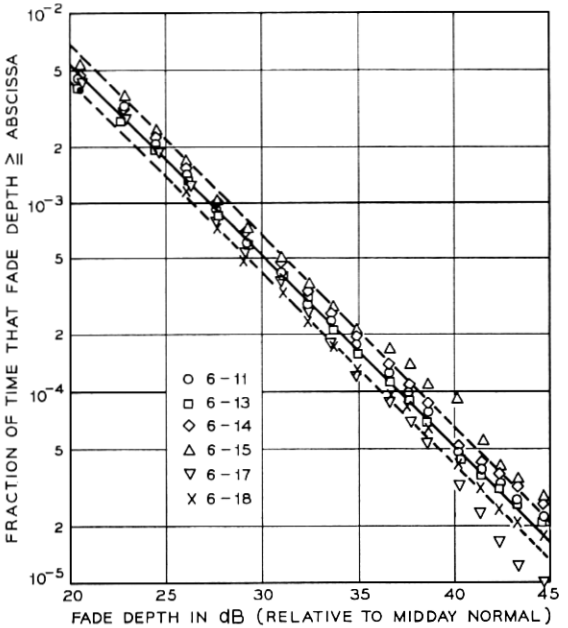

Fig. 7—Fade-depth distribution; 6-GHz channels.

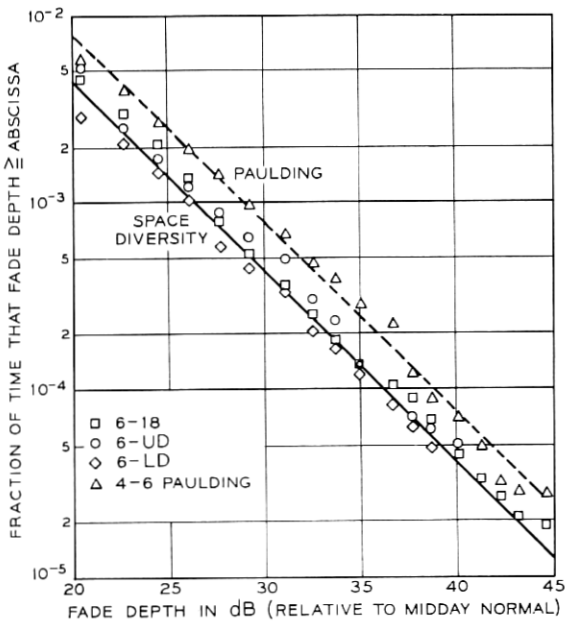

Fig. 8—Fade-depth distribution; space diversity grouping and Paulding.

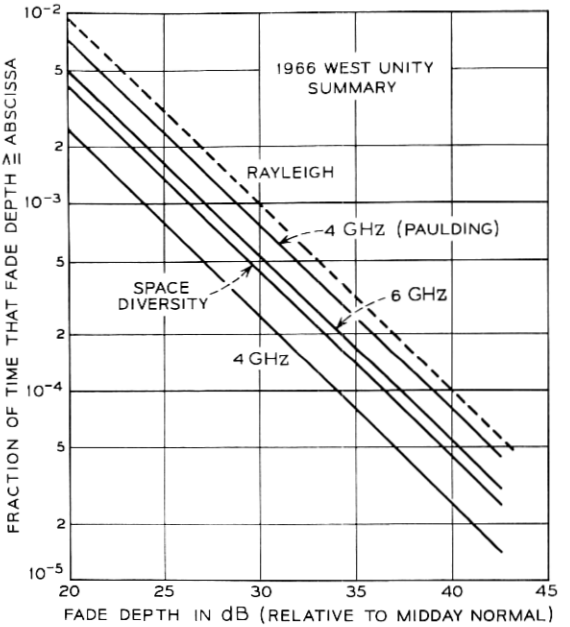

Fig. 9—Summary of fade-depth distributions.

diversity grouping (SD) and 4 GHz. The 4-GHz channels have significantly less fading than either 6-GHz (by 3.3 dB) or 4-GHz Paulding (by 4.9 dB). The 0.9-dB difference between signals on antennas of different height, that is, 6 GHz compared to SD, is thought to be more apparent than real, although it may be a small height effect.

It should be noted that having essentially the same fade distribution for the 6-18 signal as received on both the dishes and horn reflector implies two things. First, the effect of 6-GHz multimoding in the horn reflector, circular waveguide, and combining networks must be negligible because the dishes use dominant mode elliptical waveguide and no combining networks. Secondly the effect of decreased clearance at midpath for the lowest dish is less than 0.9 dB.

One way of explaining the significant differences shown on Fig. 9 is to examine them in terms of the terrain and the radio path lengths. Pearson[7] has given data taken in Britain on the relation between worst-month fading and the terrain as characterized by the path roughness.*

* Path roughness is the standard deviation of terrain height measurements at one-mile intervals on a line between transmitter and receiver with the end points of the path excluded.

Assuming that the 68-day period is equivalent to the British worst-month data, Table V can be compiled from Fig. 9 and Ref. 7.

The 6-GHz British point has been obtained by assuming that the path length is 50 percent longer at 6 GHz than it is at 4 GHz; that is, the path length is cast in terms of wavelengths.

There is good agreement between the British and the West Unity data. Thus the difference in depth of fade for a given percentage of time is apparently directly related to the terrain roughness and to the path length in wavelengths. Of course this is not sufficient evidence to justify the extensive use of these parameters. It has long been known, at least qualitatively, that fading is more severe over smooth terrain or water than on rough paths of comparable frequency, length, and atmospheric conditions.

VI. FREQUENCY DIVERSITY RESULTS

The simultaneous measurements on a number of different frequencies, together with computer processing of the differences in signal level with frequency, have provided much more quantitative information than previously available on the improvements to be expected from the use of frequency diversity. The diversity results specify the total amount of time during which the stronger of two signals was less than a certain amount (this means that both signals simultaneously were less than the given amount).

6.1 6 *GHz*

The results for the 6-GHz pairs for fade depths $\geqq$ 20 dB are given on Figs. 10 through 16. Fifteen pairs were obtained from the six 6-GHz channels and they are grouped according to frequency separations as shown in Table VI.

Four lines are shown on each figure. The uppermost is the nondiversity line which is the average single-channel fade-depth distribution as dis-

TABLE V—PATH ROUGHNESS EFFECTS

			0.1 Percent Fade Depth	
		Roughness	*British*	*West Unity*
Pleasant Lake	4 GHz	16.0 meters	23.5 dB	24.0 dB
	6 GHz	16.0 meters	29.0 dB	27.3 dB
Paulding	4 GHz	8.5 meters	28.0 dB	28.9 dB

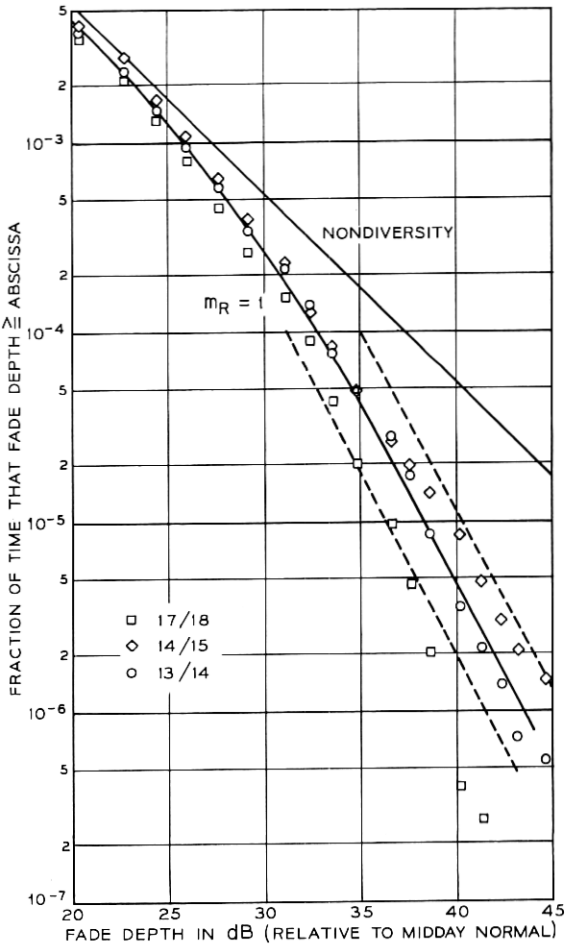

Fig. 10—6-GHz frequency diversity; 30-MHz separation.

cussed previously. The bottom solid line which is tagged with a value of a parameter m_R is a curve fitted to the data. The dashed lines are relative to the fitted line and denote a ± 2-dB corridor which is an estimate of the uncertainties in the data due to nonlinear calibration and reference value determination. The fitted curve is obtained by assuming that the diversity data is jointly Rayleigh distributed with respect to the nondiversity curve. The parameter m_R is related to the amount of correlation between the two components of the distribution. This concept will be discussed in more detail later.

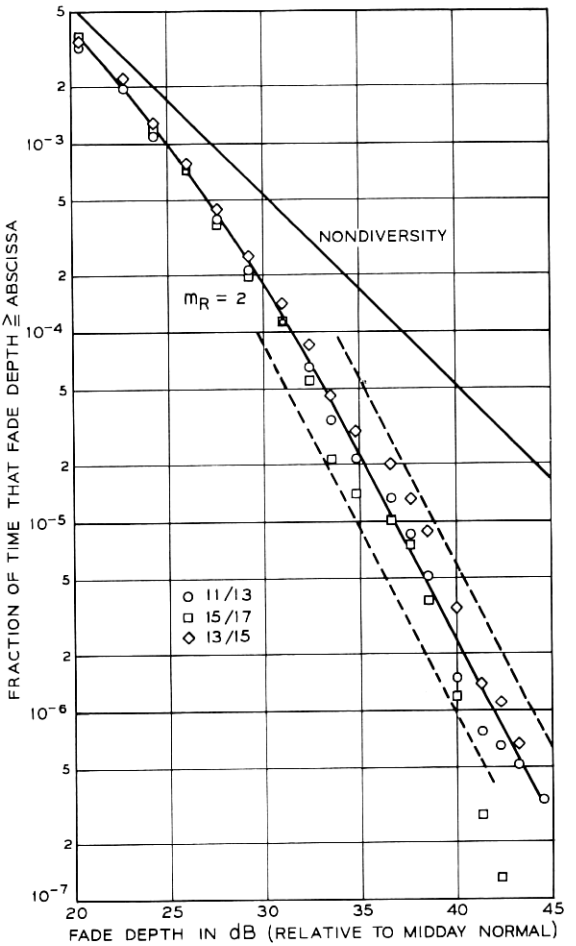

Fig. 11—6-GHz frequency diversity; 60-MHz separation.

Inspection of these results (Figs. 10 through 16) shows that for a fixed frequency separation, the scatter of the data points with respect to the fitted diversity line is small below 30-dB fade depth but increases somewhat for larger fade depths.* However for fade depths of 40 dB or less, all the data points lie within the ±2-dB corridors except for

* On the figures, 10^{-6} = 5.26 seconds which means that there were few samples at the higher fade depths.

17/18 on Fig. 10. This latter result is an anomaly because all other combinations which include 6–17 or 6–18 are quite consistent within their group. In fact, the consistency of the data points for different pairs having the same frequency separation is remarkable. Also note the excellent agreement between the data and the fitted line for the pair with the maximum frequency spacing (210 MHz).

As the frequency separation increases, it is to be expected that the

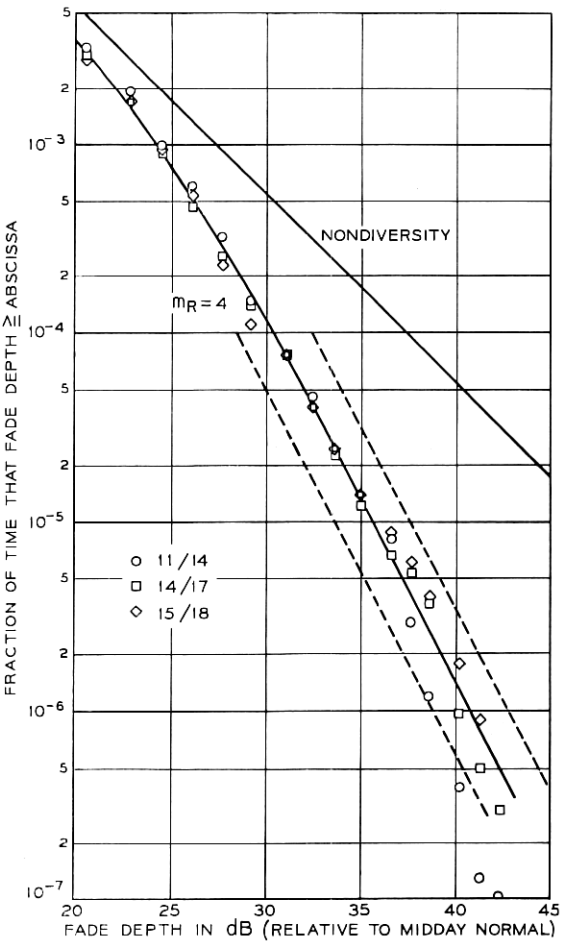

Fig. 12—6-GHz frequency diversity; 90-MHz separation.

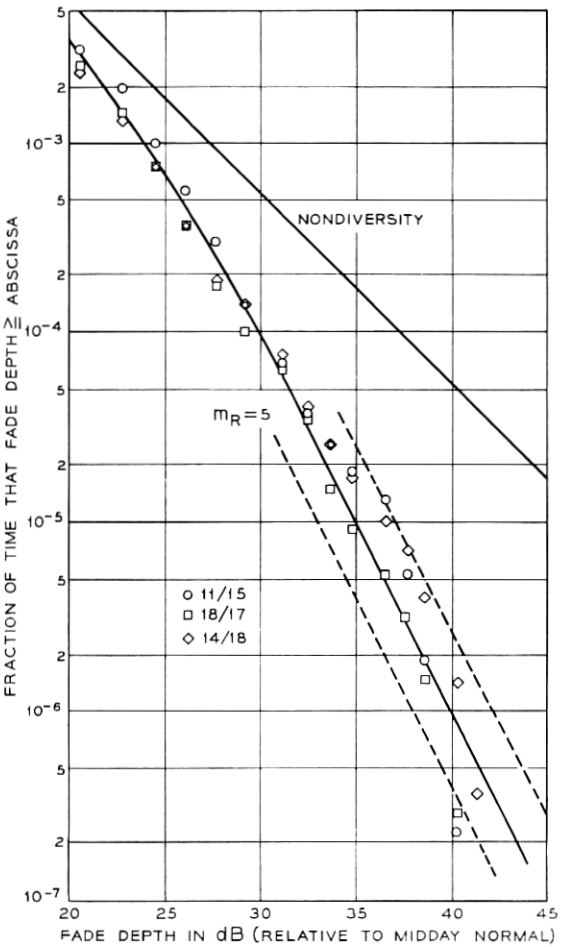

Fig. 13—6-GHz frequency diversity; 120-MHz separation.

diversity performance will improve. This is borne out on Figs. 10 through 16 and is described by increasing values of m_R for increasing frequency separation. The performance of frequency diversity relative to nondiversity will be discussed in a later section.

6.2 4 *GHz*

The results for the 4-GHz frequency diversity pairs are given on Figs. 17 through 24. Twenty-one pairs were obtained from the seven

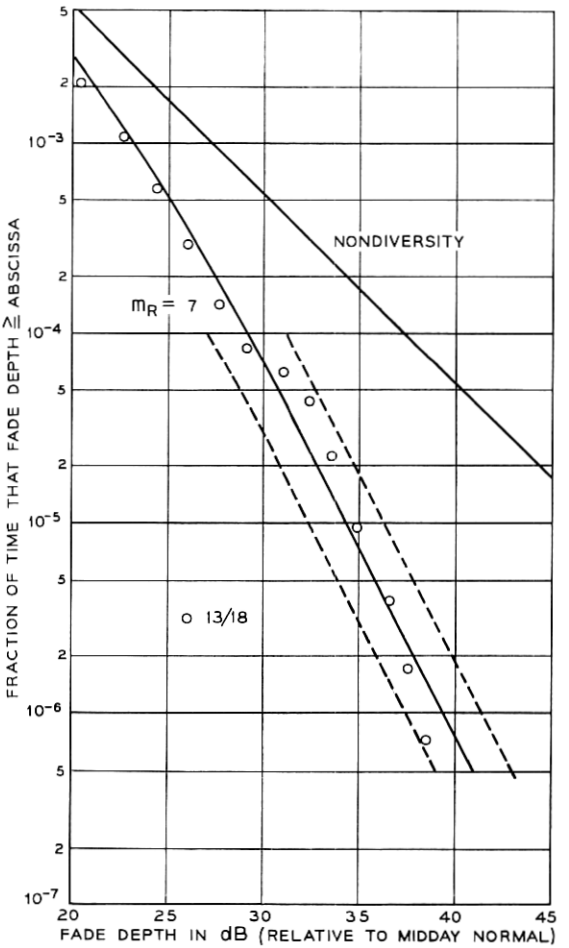

Fig. 14—6-GHz frequency diversity; 150-MHz separation.

different TD-2 channels and they are grouped according to frequency separations as shown in Table VII.

The lines on the figures have exactly the same meaning as in the 6-GHz case discussed in the previous paragraphs.

Inspection of the results shows that the scatter of the points with respect to the fitted diversity line is small for fade depths less than 30 dB except for 7/1 on Fig. 17 which has been ignored as an anomaly.

For greater fade depths, the scatter increases and the data points tend to fall off faster than the fitted line except for Fig. 23 which has a distinct upward bulge. The fast rolloff might result from noise or interference effects in the radio system. Since the 6-GHz results do not exhibit these effects, the MIDAS system and the data reduction procedures are probably not the source of this rolloff since all of the radio channels were treated identically. Further some of the pairs follow the fitted

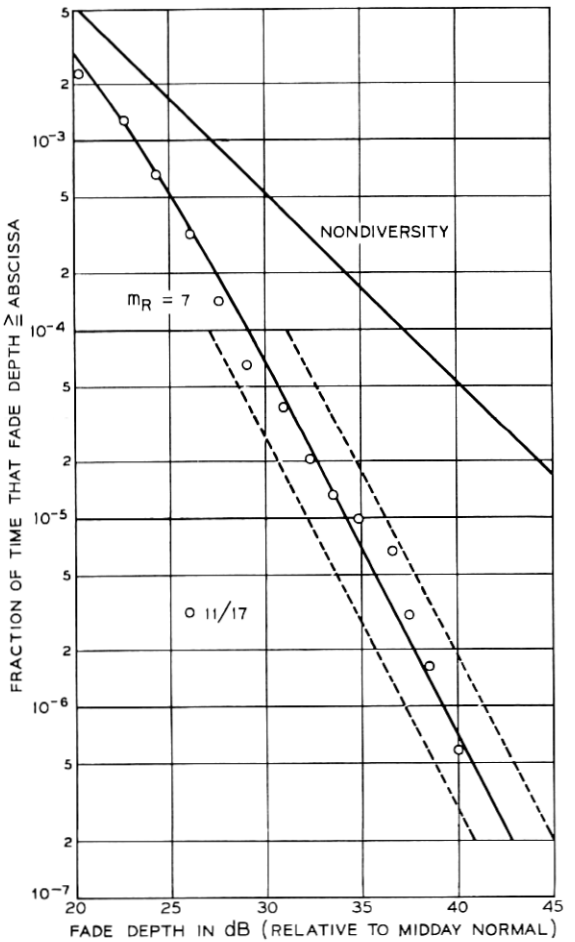

Fig. 15—6-GHz frequency diversity; 180-MHz separation.

line without any rolloff, for example, 4–9/11 on Fig. 21 and 4–7/2 on Fig. 20. The reasons for the anomalies are not explicitly known but it is assumed that they are *not* generated by multipath fading. In any case, the fitted line is a conservative approximation to the data except for Fig. 23.

Just as in the 6-GHz case when the frequency separation increases, the diversity performance improves. This is described by increasing

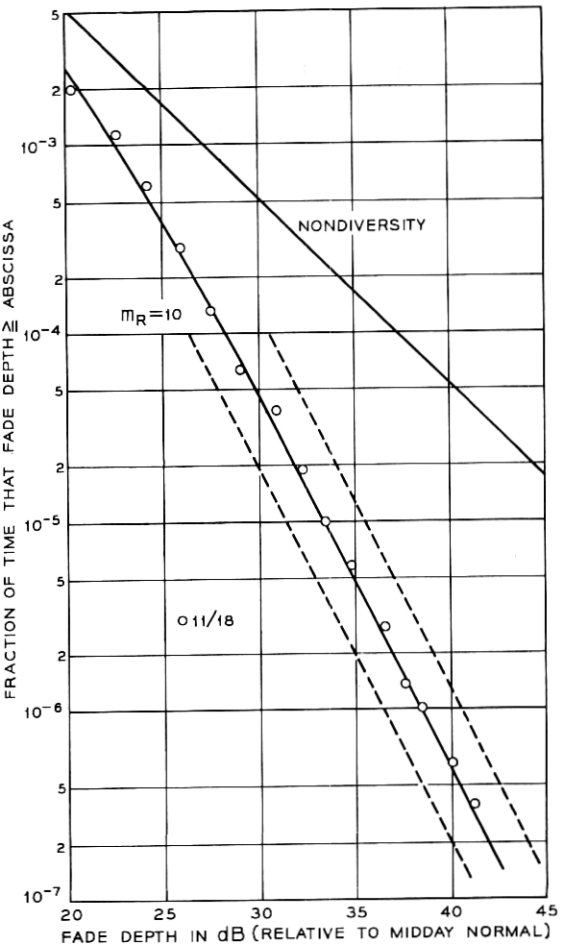

Fig. 16—6-GHz frequency diversity; 210-MHz separation.

TABLE VI—6-GHz FREQUENCY DIVERSITY RESULTS

Figure	Frequency Separation (MHz)	Number of Pairs
10	30*	3
11	60	3
12	90	3
13	120	3
14	150	1
15	180	1
16	210	1

* This is also the nominal bandwidth of the working channel.

values of m_R for increasing frequency separation and will be discussed in a later section.

VII. DESCRIPTION OF SIMULTANEOUS FADING AT DIFFERENT FREQUENCIES

Multipath fading is caused by complicated interference phenomena and it is possible that various descriptions of simultaneous fading are useful. Models for fading can be postulated on two levels. First there is a mathematical (statistical) description of the characteristics of multipath fading. Second, on a more fundamental level, there is the model for the physical process that creates fading and from which the mathematical (statistical) model could be derived. At the present time there is no physical process model which gives results that agree well with the experimental data. On the other hand, a statistical model based on the joint Rayleigh probability distribution has been useful in the description of space diversity, and it is applied here (with considerable success) to frequency diversity. However the physical process model is still the ultimate goal and the experimental data and empirical formulas presented here should aid in attaining this goal.

The following discussion briefly gives the relevant details of the joint Rayleigh distribution as applied to the data. For a Rayleigh variate, the probability that the envelope voltage R_1 of the signal normalized to its rms value has a value less than L is

$$\Pr(R_1 < L) = 1 - \exp(-L^2). \tag{1}$$

Similarly the probability distribution of the envelope voltage R_2 of a second signal normalized to the rms value of the first signal is

$$\Pr(R_2 < L) = 1 - \exp\left(-\frac{L^2}{v^2}\right) \tag{2}$$

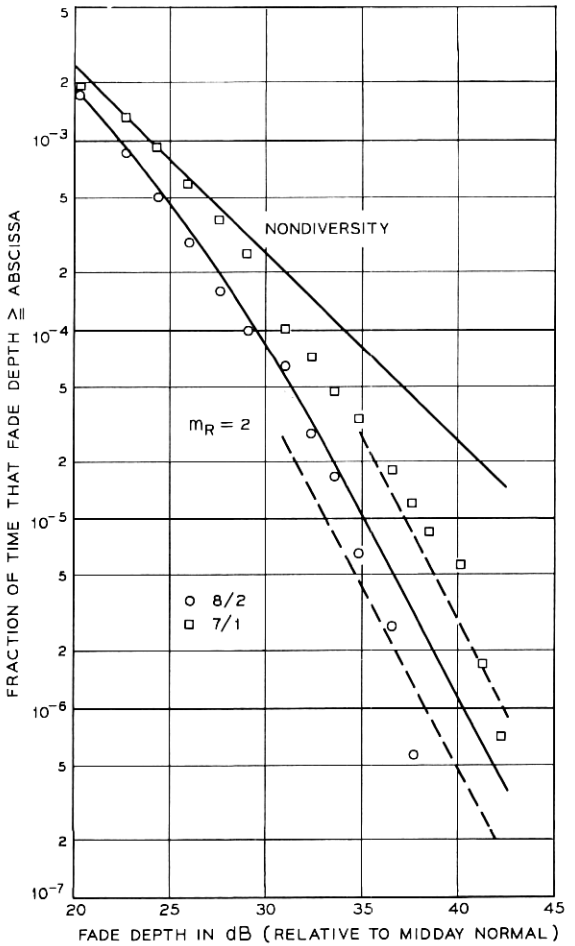

Fig. 17—4-GHz frequency diversity; 20-MHz separation.

where

$$v^2 = \langle R_2^2 \rangle_{av} (\langle R_1^2 \rangle_{av})^{-1}. \tag{3}$$

The joint probability distribution function of the variables R_1 and R_2 is[10]

$$\Pr(R_1 < L, R_2 < L) = \int_0^{L^2/(1-k^2)} dX_1 \int_0^{(L/v)^2/(1-k^2)} dX_2 P(X_1, X_2) \tag{4}$$

with

$$P(X_1, X_2) = (1 - k^2)I_0[2k(X_1X_2)^{1/2}] \exp[-(X_1 + X_2)$$

where k^2 is the correlation coefficient of R_1^2 and R_2^2. For use in this paper m_R has been defined as

$$m_R = 10^3(1 - k^2). \tag{5}$$

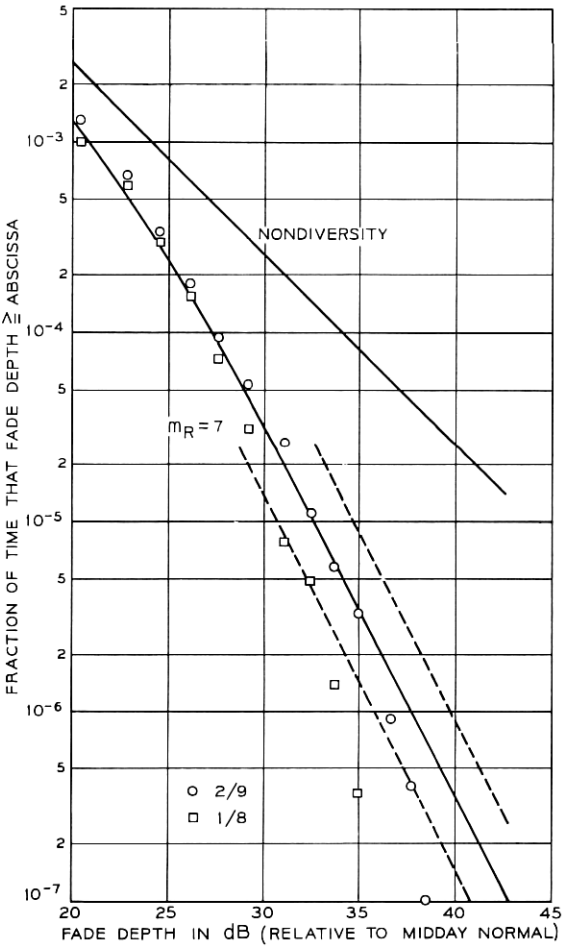

Fig. 18—4-GHz frequency diversity; 60-MHz separation.

Typical computed results are shown in Fig. 25 for $v^2 = 1$. For deep fades, asymptotic forms of equations (2) and (4) are quite useful.

$$\Pr(R_2 < L) \cong L^2 v^{-2} \tag{6}$$

and

$$\Pr(R_1 < L, R_2 < L) \cong (10^3/m_R)(L^4/v^2). \tag{7}$$

The region of validity of equations (6) and (7) depends on v, L, and m_R .

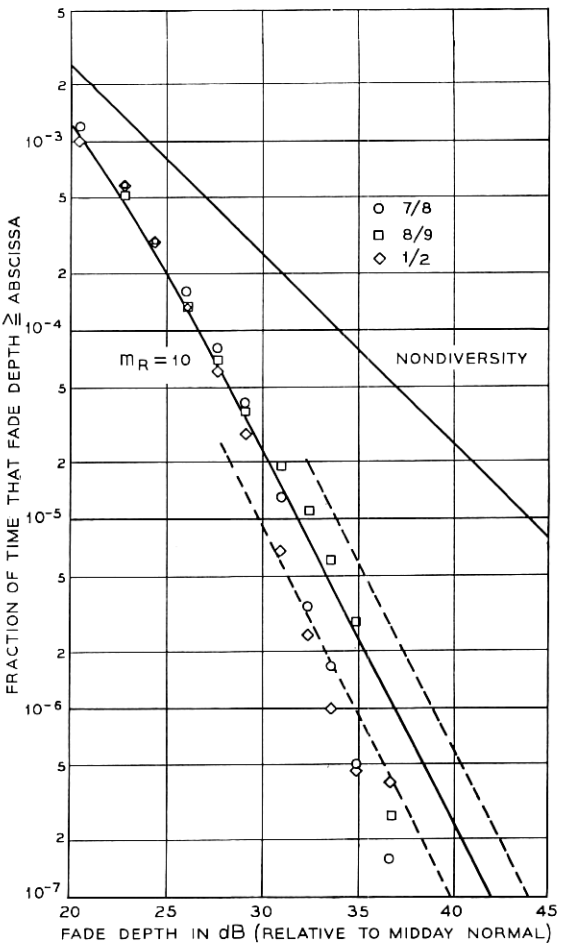

Fig. 19—4-GHz frequency diversity; 80-MHz separation.

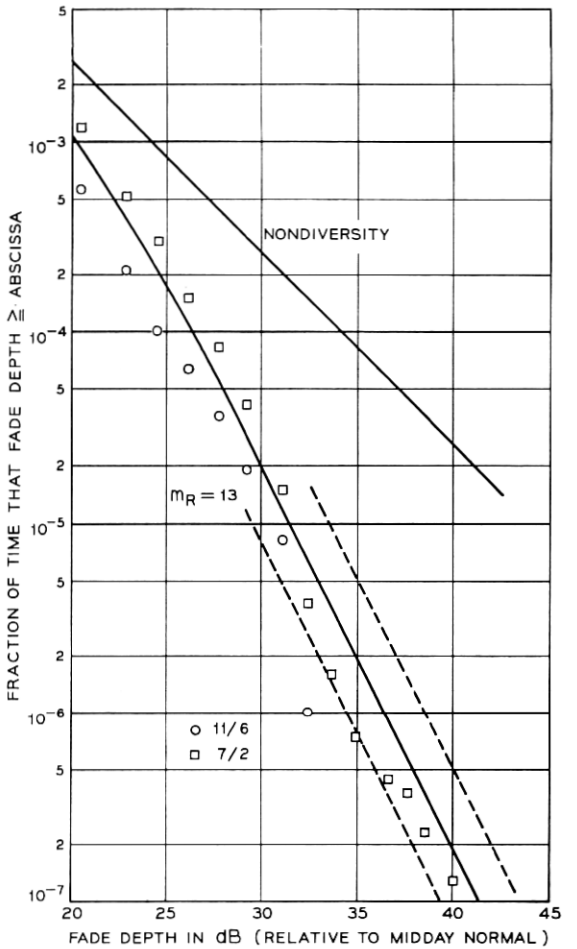

Fig. 20—4-GHz frequency diversity; 100-MHz separation.

For example it is the region in Fig. 25 where the lines are parallel to the $m_R = 10^3$ line.

The joint Rayleigh distribution, calculated from equation (4), was fitted to the diversity data points by overlaying plots of the joint distribution for various values of m_R and choosing the one with the best apparent fit. The results of this are the bottom solid lines on the diversity plots with the value of m_R next to each line. In the fitting, somewhat

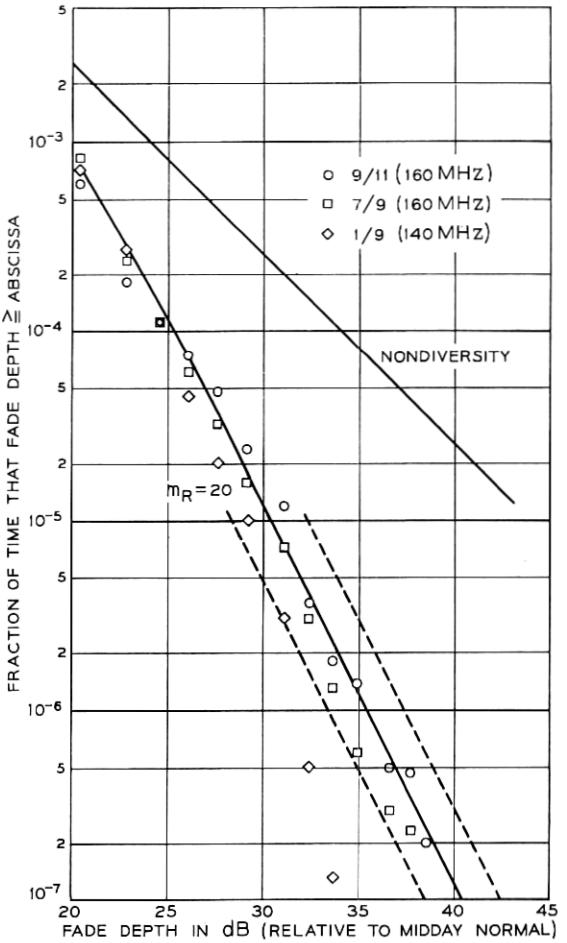

Fig. 21—4-GHz frequency diversity; 140/160-MHz separation.

more weight was given to the values at 30-dB fade rather than at 40 dB because of relative sample size. Also note that the curvature of the joint Rayleigh fits the curvature of the data points for the smaller fade values.

VIII. IMPROVEMENT

The quantity of interest in any diversity scheme is the amount of improvement relative to the nondiversity performance. Here this per-

formance measure is defined as the ratio of fractional outage of the nondiversity signal to that of the diversity signal for a fixed fade depth. Description by this factor (I) is convenient because it avoids detailed description of the many schemes that are used to process the two signals. The best of these switching or combining schemes will provide performance equal to or somewhat better than that described by the fade reduction factor.

The fraction of the total time that a nondiversity signal is faded

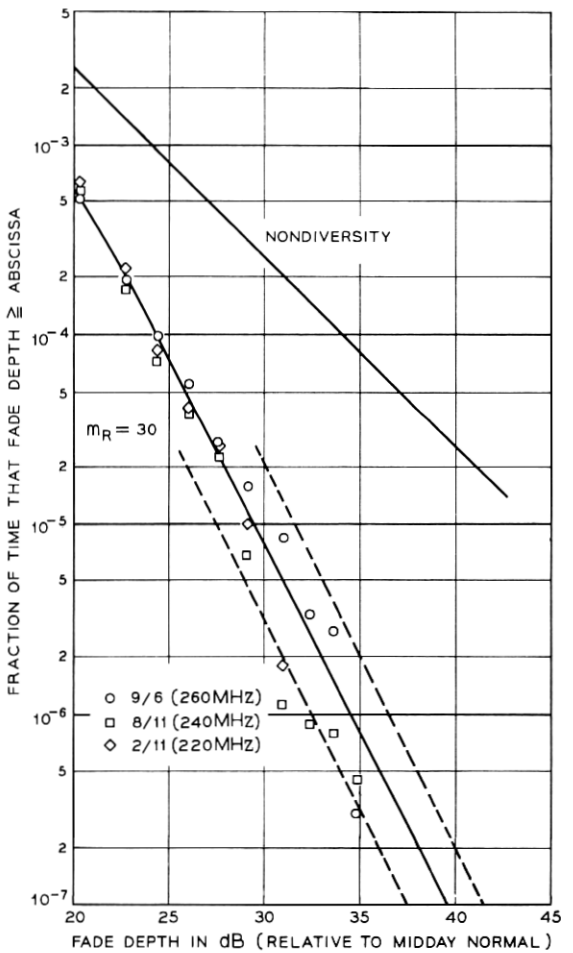

Fig. 22—4-GHz frequency diversity; 220/240/260-MHz separation.

depends on frequency, path length, terrain, antenna placement, and climate. The last of these determines the fraction of the total time that fading conditions exist on a given path. The periods used in analysis were those for which fading conditions were in existence. Any change in the total time of such fading periods would have no effect on the statistics since they pertain to the fading phenomena and not to the length of time (assuming an adequate number of samples are available). However, the statistics have been normalized by adding in the remaining

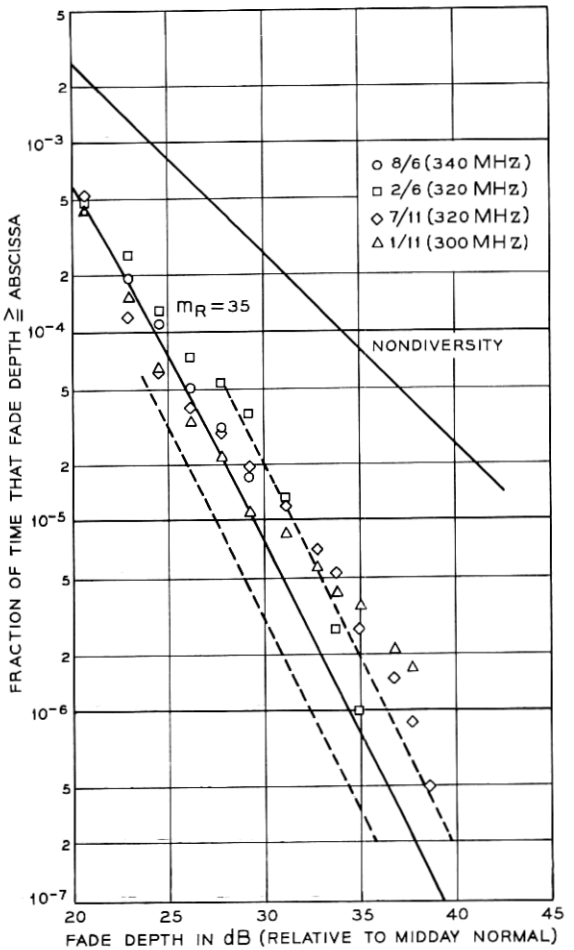

Fig. 23—4-GHz frequency diversity; 300/320/340-MHz separation.

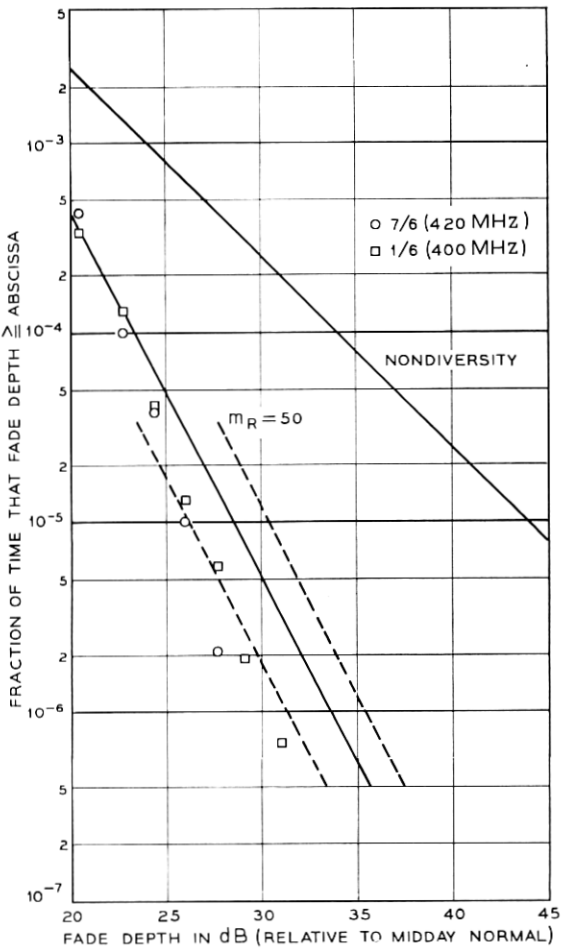

Fig. 24—4-GHz frequency diversity; 400/420-MHz separation.

or nonfading time. The effect of this or any like change in the amount of the nonfading time is a uniform shift in the nondiversity and diversity curves without changing their shape or their ratio; that is, the fractional time scale is multiplied by a constant. This last fact has been heavily utilized in the analysis where this ratio has been called the improvement factor (I). Note that the improvement factor does not depend on how often fading conditions exist but rather upon what happens within these selective fading periods.

TABLE VII—4-GHz FREQUENCY DIVERSITY RESULTS

Figure	Frequency Separation (MHz)	Number of Pairs
17	20*	2
18	60	2
19	80	3
20	100	2
21	140	1
	160	2
22	220	1
	240	1
	260	1
23	300	1
	320	2
	340	1
24	400	1
	420	1

* This is also the nominal bandwidth of the working channel.

Referring to the asymptotic forms for the joint Rayleigh model, equations (6) and (7), the asymptotic form of the improvement factor (I) for Rayleigh fading can be stated as

$$I = \frac{\Pr(R_1 < L)}{\Pr(R_1 < L, R_2 < L)} = \frac{(m_R/10^3)}{\Pr(R_1 < L)} \tag{8}$$

where, for the time being, it is assumed that both signals have the same rms value (that is, $v^2 = 1$).

The experimental improvement factors were obtained from the ratio between the fitted diversity line and the nondiversity lines for the 6-GHz and 4-GHz frequency pairs at a 40-dB fade depth. The values are plotted on Fig. 26 versus the parameter $\Delta f/f$. Here f is taken as 3950 MHz for the 4-GHz band and 6175 MHz for the 6-GHz band and Δf is the average frequency separation for a grouping on a single figure, for example, $\Delta f = 240$ MHz for Fig. 22. If the $\pm$2-dB uncertainty were included, the points plotted on Fig. 26 would change to vertical lines between 1.58 and 1/1.58 of the average value shown. Even with this large range of uncertainty, it appears that the improvement and $\Delta f/f$ are linearly related as shown by the lines on the figure. The equations of the lines are

$$\left.\begin{aligned} &4\text{ GHz: } I = \frac{1}{2}\left(\frac{\Delta f}{f}\right)L^{-2} \text{ for } I \geqq 10, \quad \text{good accuracy;} \\ &6\text{ GHz: } I = \frac{1}{4}\left(\frac{\Delta f}{f}\right)L^{-2} \text{ for } 1 \leqq I \leqq 10, \quad \text{less accurate but conservative;} \end{aligned}\right\} \tag{9}$$

where $F = -20 \log L$ is the fade depth in dB. This is the asymptotic form of the formulas including the variation with fade depth as shown in equation (8).

Using equation (8) as a guide, it is conjectured that the experimental improvement can be separated into two parts which contain respectively the nondiversity fading and the frequency diversity effect, that is,

$$I = \frac{m/10^3}{P(L)} \tag{10}$$

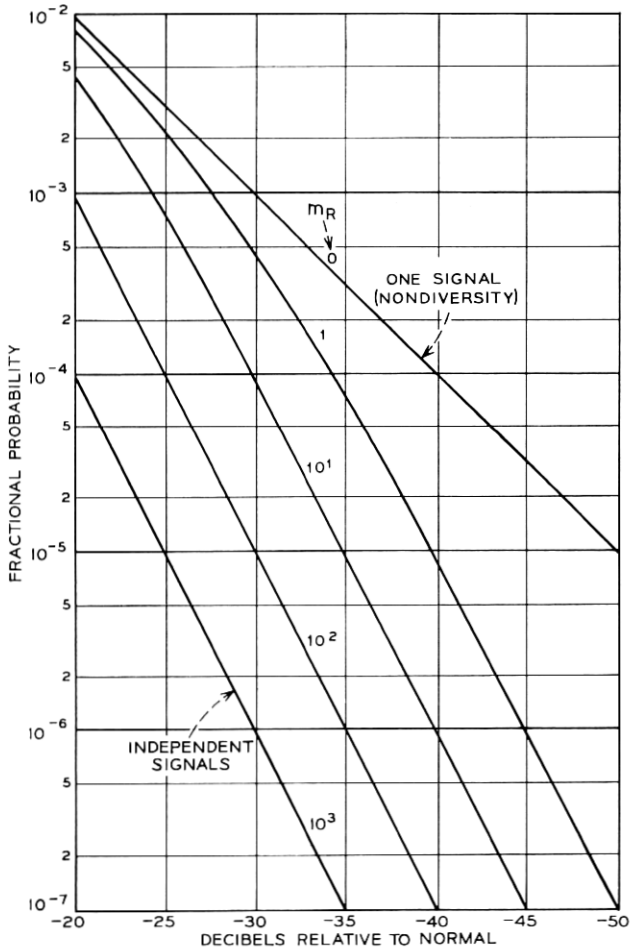

Fig. 25—Probability that both signals are simultaneously less than a given amount (Joint Rayleigh Distribution).

where $P(L)$ is the measured probability that a nondiversity fade exceeds $-20 \log L$ dB and m is a frequency diversity parameter. Of course both these quantities are functions of frequency, path geometry, terrain, and antenna placement.

Consider first the variation of m with $\Delta f/f$ and secondly the difference in improvement between the 4-GHz and 6-GHz bands.

The nondiversity results $[P(L)]$ can be written as (see Fig. 9)

$$\begin{aligned} 6 \text{ GHz:} \quad & P_6 = (.53)L^2, \\ 4 \text{ GHz:} \quad & P_4 = (.25)L^2, \end{aligned} \tag{11}$$

where $F = -20 \log L$ is the fade depth in dB. Then from equations (9) and (10)

$$\begin{aligned} 6 \text{ GHz:} \quad m_6 &= (10^3)\left(\frac{1}{4}\right)\left(\frac{\Delta f}{f}\right)L^{-2}(.53)L^2, \\ &= 132.5\,\frac{\Delta f}{f}\,; \end{aligned} \tag{12}$$

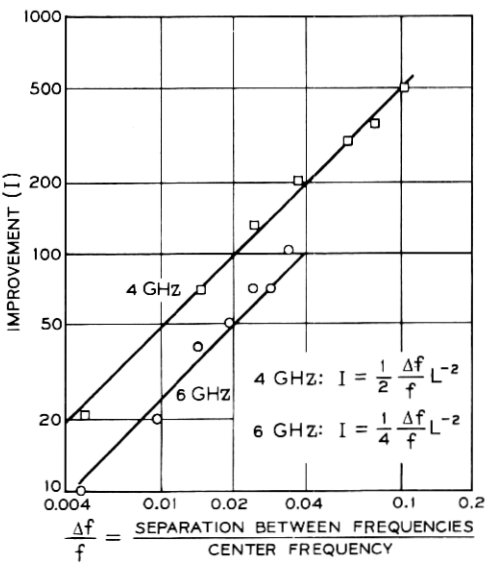

Fig. 26—1966 West Unity in-band frequency diversity improvement ratio at 40-dB Fade Depth ($L = 0.01$).

$$\begin{aligned} 4 \text{ GHz:} \quad m_4 &= (10^3)\left(\frac{1}{2}\right)\left(\frac{\Delta f}{f}\right)L^{-2}(.25)L^2, \\ &= 125\,\frac{\Delta f}{f}\,. \end{aligned} \tag{13}$$

The difference between m_6 and m_4 is small. Thus as desired m depends primarily upon normalized frequency spacing and not upon either the nondiversity fading distribution or the radio frequency band (4 vs 6 GHz). For further use it is assumed that $m = 130\ \Delta f/f$.

Using equations (9) and (10) again and forming a ratio gives

$$\frac{I_4}{I_6} = \frac{P_6}{P_4} = 2.1 \tag{14}$$

which agrees very closely with the experimental ratio of 2 shown on Fig. 26. Thus equation (10) correctly predicts the relative improvement between the 6- and 4-GHz bands. Further this relative improvement depends upon the nondiversity fading results and not upon the normalized frequency spacing.

To recapitulate, the asymptotic value of improvement of an in-band frequency diversity pair relative to the nondiversity signal at a fade depth of $-20 \log L$ dB can be stated for the experimental data as

$$I = \frac{0.13\,\dfrac{\Delta f}{f}}{P(L)} \tag{15}$$

where $P(L)$ is the probability that the nondiversity signal fades below the given depth. In this formula, I is not affected by the relative amount of time that fading conditions do or do not exist. However both the numerator and denominator in equation (15) would change by the same multiplicative constant when the ratio of nonfading to fading time changes. Thus the terms $P(L)$ and $0.13\ \Delta f/f$ individually apply only to the experimental path but their ratio is more generally useful.

This ratio (I) characterizes frequency diversity during multipath fading periods. Although I was obtained from experimental data on one path, it should pertain to other paths of about the same length but having different terrain and climate. The terrain and climate play a major role in determining the fraction of time that multipath fading conditions exist but they probably will have only a secondary effect on the relation between a nondiversity signal and a diversity signal within a multipath fading period.

IX. CROSSBAND FREQUENCY DIVERSITY

Results were also obtained for a subset of the 4-GHz and 6-GHz channels where the diversity pair consists of one channel from each group. The channels used for analysis were 4-2, 4-1, 4-7, 4-6 and 6-11, 6-15, 6-18. The results are given in Figs. 27 through 30. The groupings for each figure are for one of the 4-GHz channels in diversity with each of the 6-GHz channels. As before, there are several curves on each figure. The two uppermost are the average nondiversity results for each band with the 6 GHz being 3.3 dB poorer than the 4 GHz for a fixed probability.

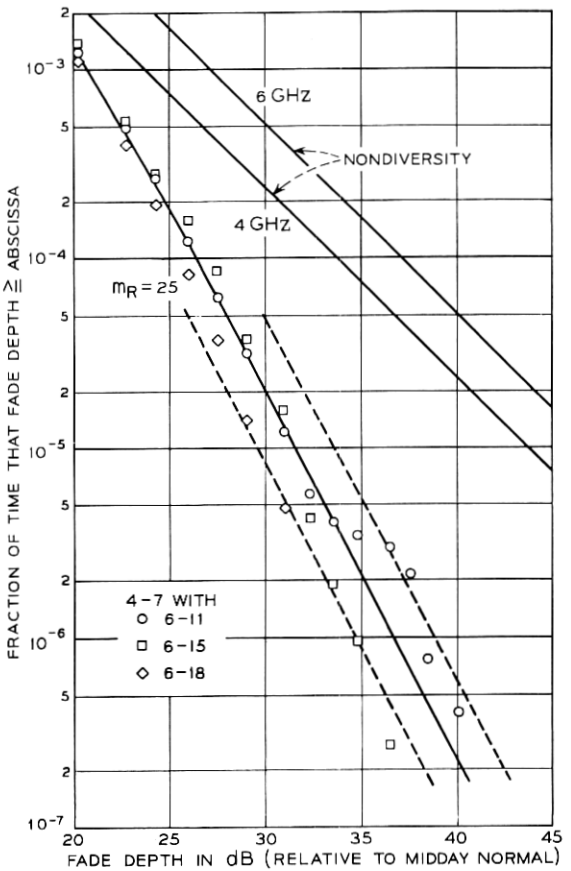

Fig. 27—4/6-GHz crossband frequency diversity.

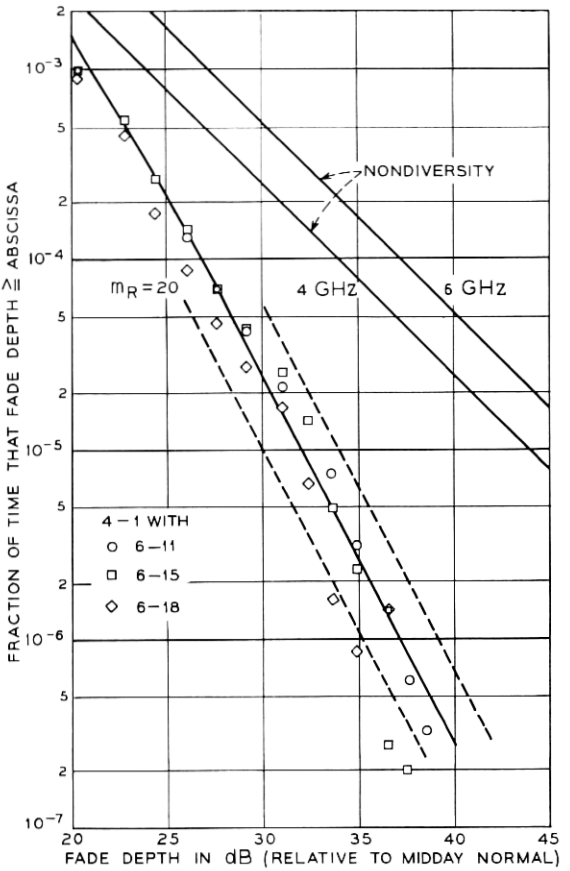

Fig. 28—4/6-GHz crossband frequency diversity.

Again the joint Rayleigh distribution was fitted to the data by overlaying plots of the joint distribution for various values of m_R. In this case the rms values are unequal by an amount

$$-10 \log v^2 = 3.3 \text{ dB} \tag{16}$$

or

$$v^2 = 0.47.$$

The asymptotic form of the improvement factor I between the diversity curve and the top nondiversity curve (6 GHz) is given as in equation (8)

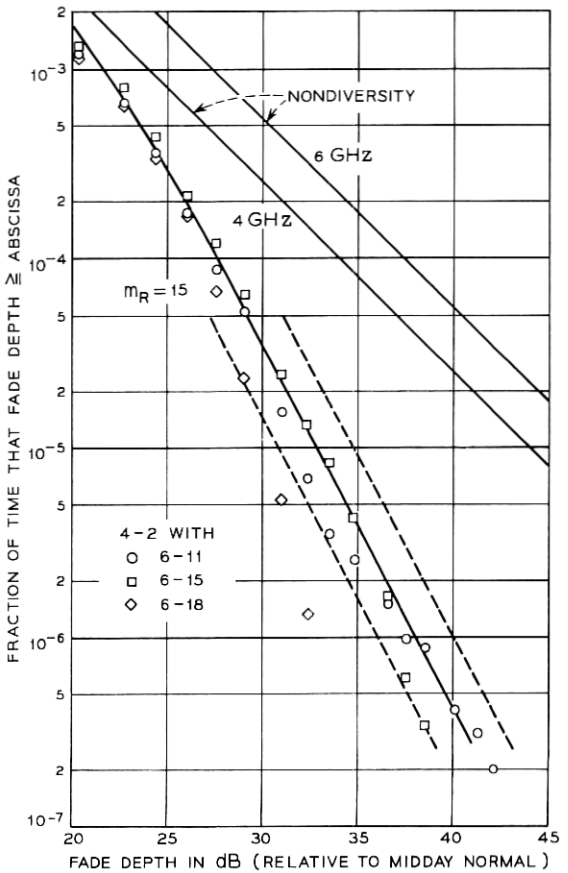

Fig. 29—4/6-GHz crossband frequency diversity.

by

$$I_{\max} = \frac{m_R/10^3}{\Pr(R_1 < L)}. \tag{17}$$

This corresponds to the improvement obtained if a 4-GHz channel were used to protect a 6-GHz channel.

The asymptotic ratio between the bottom nondiversity curve (4 GHz) and the diversity curve is then

$$I_{\min} = v^2 \frac{m_R/10^3}{\Pr(R_1 < L)} = v^2 I_{\max} \tag{18}$$

which corresponds to the improvement obtained if a 6-GHz channel were used to protect a 4-GHz channel. In these formulas, m_R and Pr $(R_1 < L)$ are Rayleigh quantities with m_R related to the correlation coefficient and $-20 \log L$ equal to the fade depth in dB exceeded by the envelope voltage R_1.

Inspection of the results shows that the points have more scatter than the 6-GHz in-band diversity data and just about the same scatter as the 4-GHz in-band diversity data, that is, the fitted line is a good representation of the data from 20 to 30 dB with increasing divergence for greater fade depths.

As to quantitative interpretation, the results do not appear to be as

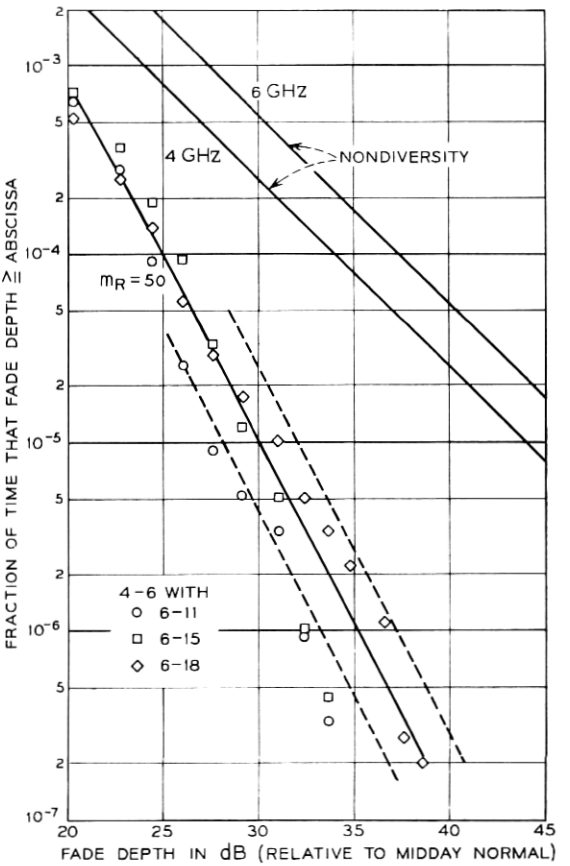

Fig. 30—4/6-GHz crossband frequency diversity.

yielding to analysis as the in-band diversity. This may result because the frequency spacings are a significant percentage of the average center frequency, for example, spacings of 1775 MHz (4-6/6-11) to 2405 MHz (4-7/6-18). The improvement values obtained from the fitted lines on the figures at 40-dB fade depth are presented in Table VIII.

The results do not show a consistent behavior as a function of frequency separation. 4-7, which has the largest frequency separation, shows slightly more improvement than 4-1 or 4-2 but less than 4-6 which has the smallest frequency separation. However, 4-2, 4-1, 4-7 are tightly bunched in frequency whereas 4-6 is about 300 MHz closer to the 6-GHz band.

In any case, these results are comparable to the in-band diversity results, that is, the improvement from crossband diversity was not significantly better than in-band diversity of two percent or more separation. Thus there may be a saturation effect which will appear for frequency separations above say 10 percent. There is neither enough data nor a theory to prove or disprove such speculation.

X. CROSS ROUTE DIVERSITY

Diversity results were obtained for various 4-GHz and 6-GHz channels on the Pleasant Lake hop in diversity with the single 4-GHz channel measured on the Paulding hop. The previous data strongly implies that it may be very misleading to rely on the results for a single channel. However, this data is included for completeness. To review: the Paulding data is for a *different* path but for the same time periods. One would therefore expect the diversity performance to be very good since the signals from the pair of paths should be reasonably independent. However this did not appear to be the case.

The data are shown in Figs. 31 and 32 in the groupings presented in Table IX. The lines on the figure have exactly the same meaning as the corresponding ones in the crossband section. In this case the 6-GHz fit

TABLE VIII—CROSSBAND IMPROVEMENT VALUES

	I_{max}	I_{min}*
Fig. 27	250	125
Fig. 28	200	100
Fig. 29	150	75
Fig. 30	500	250

* $I_{min} = v^2 I_{max}$ from equation (16) with $v^2 = 0.47$ but 0.5 has been used in this table for convenience.

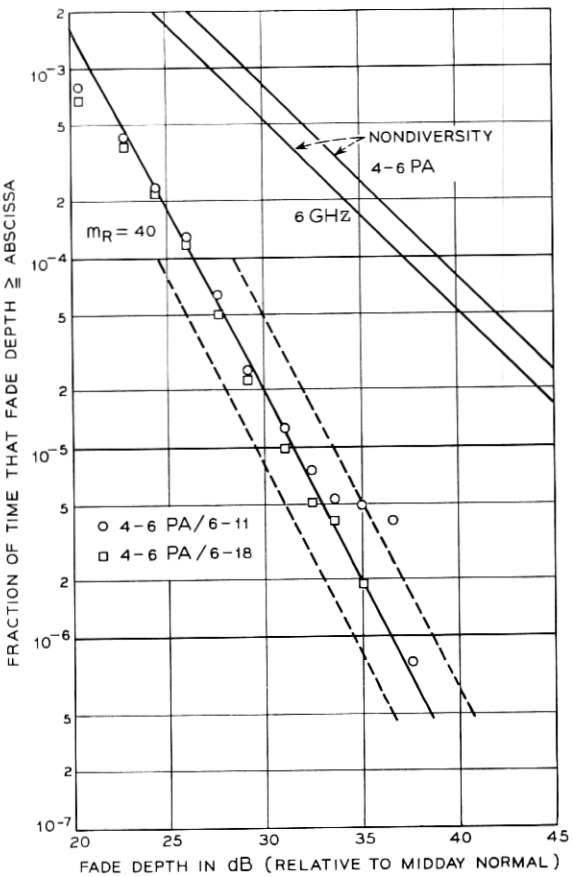

Fig. 31—4/6-GHz cross route diversity.

is good but the 4-GHz fit is poor below 30 dB in that the data has an upward bulge. There is no explanation available for this anomaly.

In any case, the improvement obtained when the two channels in the diversity pair are on different hops is not significantly better than in-band diversity (see Fig. 26). This is surprising and raises questions about the correlation between fading on adjacent hops, for example, the maximum possible diversity improvement may be limited to values less than that expected from independent fading.

To repeat, this is based on a single channel and as such the data base

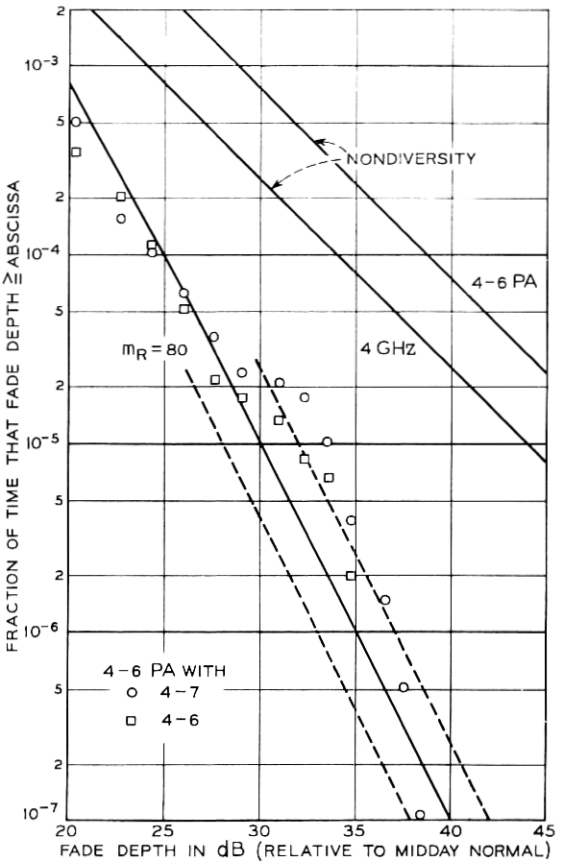

Fig. 32—4-GHz cross route diversity.

TABLE IX—CROSS-ROUTE RESULTS

Figure	Diversity Pairs	I_{max}	I_{min}*
31	6-11 with 4-6 PA 6-18 with 4-6 PA	400	300
32	4- 7 with 4-6 PA 4- 6 with 4-6 PA	800	250

* $I_{min} = v^2 I_{max}$
4/4-PA, $v^2 = 0.322$ (used 0.31)
6/4-PA, $v^2 = 0.715$ (used 0.75)

is simply not sufficient to draw any profound conclusions about cross-route effects.

XI. COMPARISON OF FREQUENCY AND SPACE DIVERSITY IMPROVEMENT

The empirical results for space diversity given in Vigants[10] can be compared with those obtained here for frequency diversity. The improvement factor for space diversity is

$$I_{SD} = \frac{s^2}{2.75D\lambda} 10^{F/10} \tag{19}$$

where

s is vertical separation between equal antennas in feet,
D is path length in feet,
λ is wavelength in feet, and
F is fade depth in dB.

Using $D = 28.5$ miles and equation (9) gives the various diversity improvement factors as presented in Table X.

These are plotted in Fig. 33 for a fade depth of 40 dB. Several points are immediate. First the improvement increases with frequency for space diversity and decreases with frequency for frequency diversity; that is, space diversity becomes relatively more effective as the operating frequency increases. The maximum improvement for frequency diversity is 100 for the maximum allowable spacing of 4 percent in the standard 6-GHz frequency plans. Space diversity of 26 feet will give this improvement. Since this spacing is reasonable, it can be said that space diversity is "better" than frequency diversity at 6 GHz. At 4 GHz, the corresponding values are $I = 625$ for 12.5 percent and 79′ spacings. In this case, frequency and space diversity are comparable in performance.

These comparisons have been made only for one-for-one space and frequency diversity on a single hop; additional data and studies are needed to clarify our understanding.

TABLE X—DIVERSITY IMPROVEMENT FACTORS

	4 GHz	*6 GHz*
Frequency	$0.5(\Delta f/f)10^{F/10}$	$0.25(\Delta f/f)10^{F/10}$
Space	$(s^2/10^5)10^{F/10}$	$1.5(s^2/10^5)10^{F/10}$

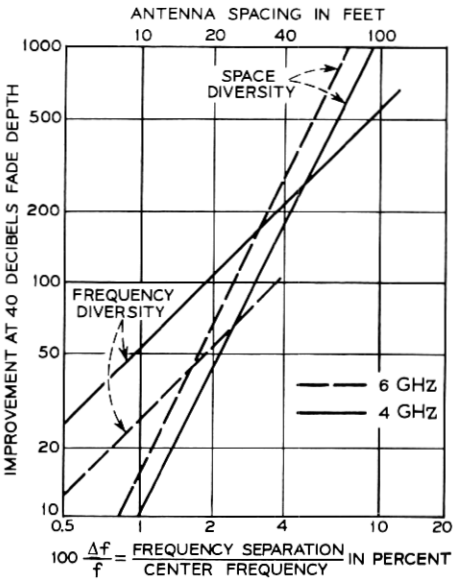

Fig. 33—Comparison of space and frequency diversity at a 40-dB fade depth.

XII. ACKNOWLEDGMENTS

The author is indebted to colleagues at Bell Telephone Laboratories for the experimental data and for many discussions. In particular the MIDAS is the creation of G. A. Zimmerman. The tabulated data used here was extracted from the raw data through the skilled labors of C. H. Menzel. There were many fruitful discussions with A. Vigants, and the interest and support of K. Bullington were invaluable.

REFERENCES

1. Kerr, D. E., *The Propagation of Short Radio Waves*, MIT Radiation Lab. series No. 13, New York: McGraw-Hill, 1951.
2. Crawford, A. B., and Jakes, W. C., "Selective Fading of Microwaves," B.S.T.J., *31*, No. 1 (January 1952), pp. 68–90.
3. De Lange, O. E., Propagation Studies at Microwave Frequencies by Means of Very Short Pulses," B.S.T.J., *31*, No. 1 (January 1952), pp. 91–103.
4. Sharpless, W. M., "Measurement of the Angle of Arrival of Microwaves," Proc. I.R.E., *34*, No. 11 (November 1946), pp. 837–845.
5. Crawford, A. B., and Sharpless, W. M., "Further Observations of the Angle of Arrival of Microwaves," Proc. I.R.E., *34*, No. 11 (November 1946), pp. 845–848.
6. Yonezawa, S., and Tanaka, N., *Microwave Communication*, Tokyo: Maruzen Co., Ltd., 1965, pp. 25–60.

7. Pearson, K. W., "Method for the Prediction of the Fading Performance of a Multisection Microwave Link," Proc. IEEE, *112*, No. 7 (July 1965), pp. 1291–1300.
8. Beckmann P., and Spizzichino, A., *The Scattering of Electromagnetic Waves from Rough Surfaces*, New York: Pergamon Press, 1963, pp. 355–367.
9. Kaylor, R. L., "A Statistical Study of Selective Fading of Super High Frequency Radio Signals," B.S.T.J., *32*, No. 5 (September 1953), pp. 1187–1202.
10. Vigants, A., "Space Diversity Performance as a Function of Antenna Separation," IEEE Trans. Comm. Tech., *COM-16*, No. 6 (December 1968), pp. 831–836.